

Thermophysical Properties of Porous Sandstones: Measurements and Comparative Study of Some Representative Thermal Conductivity Models

A. Maqsood^{1,2} and K. Kamran¹

Received October 16, 2004

The thermal conductivity and thermal diffusivity of porous consolidated sandstones have been measured simultaneously by the transient-plane source (TPS) technique in the temperature range from 280 to 330 K at ambient pressure using air as the saturant. The porosity and density parameters are measured using standard American Society for Testing and Materials (ASTM) methods at 307 ± 1 K. Data are presented for five types of samples ranging in porosity from 8 to 17 vol.%, taken from various positions above the baseline. The thermal conductivity and constituents of the minerals vary with porosity as well as with the position of the sample from the baseline. The thermal conductivity data are discussed in the framework of simple mixing laws and empirical models. Simple correlations between the effective density and porosity, and between the effective thermal conductivity and porosity, are also established.

KEY WORDS: density; mixing law models; porosity; sandstone; thermal conductivity; thermal diffusivity; transient plane source (TPS) technique.

1. INTRODUCTION

The most relevant thermal parameters of rocks are the thermal conductivity, heat capacity, and thermal diffusivity. The first two parameters give the capability of a material to conduct and accumulate heat, respectively, and the last one gives an estimate of what area of the material has been affected by the amount of heat per second. A knowledge of

¹ Thermal Physics Laboratory, Department of Physics, Quaid-i-Azam University, Islamabad 45320, Pakistan.

² To whom correspondence should be addressed. E-mail: tpl@qau.edu.pk or tpl.qau@usa.net

the thermal transport properties of rocks as a function of temperature has become important with the widespread interest in thermal processes, e.g., underground fluid-bearing reservoirs. Some of these processes include thermal methods of enhanced oil recovery, management of geothermal reservoirs, and underground disposal of nuclear waste.

The design of thermal-insulating materials depends upon the heat transfer characteristics of porous media. The thermal conductivity of a given piece of rock depends, at constant temperature and pressure, on the mineralogical composition as well as on its porosity and pore filling (which can be air, water, oil, etc.) and also on the geometrical composition.

The present work presents thermal parameters of five porous sandstones taken from various positions from the base of Khewra sandstones located in the north of Pakistan. The porosity, density, and mineral compositions of the samples were determined, and the effect of these parameters on the effective thermal conductivity has been investigated. The variation of thermal conductivity and thermal diffusivity in the temperature range from 280 to 330 K is also reported.

2. THEORIES

2.1. Thermal Conductivity Prediction Models

Precise measurements of thermal conductivities of rocks are difficult to conduct and can be very time-consuming. To make laboratory measurements on all types of rock of interest and under all environmental conditions of temperature, pressure, and fluid saturation would be prohibitive in terms of time and expense. Consequently, a great deal of effort has gone into the development of models relating thermal properties and behavior to more easily measured properties (such as porosity, density, etc.) of rock/fluid systems. These models often predict thermal conductivities within 20%. By using these models, it is also possible to tailor [1] the materials for a specific application.

A large number of expressions [2–6] have been developed for prediction of the effective thermal conductivity of multiple-phase porous materials. Most of them, originally developed for two-phase systems, have been extended to three-phase systems.

Existing models can be classified into three major categories. The first type involves the application of the mixing laws for porous mineral aggregates containing various fluids. Since these models do not take into account the structural characteristics of rocks, they are of limited applicability. A second type is the empirical model in which more easily measured physical properties are related to thermal conductivity

through the application of regression analysis to laboratory data. One can distinguish between semi-empirical and empirical relationships; the former do not include any adjustable parameters, whereas the latter include such parameters [5, 7] and thus some thermal conductivity measurements are required. This method also has its shortcomings in that the resulting model may be applicable only to the particular suite of rocks being investigated. The third type is a theoretical model based on the mechanism of heat transfer applicable to simplified geometries of the rock/fluid system. In the literature, efforts in this direction have been published [6, 8–16]. The two models proposed to date have limited applicability and cannot be used for all types of systems, especially when the difference in the thermal conductivities of the constituent phases is very large. A general expression to predict the effective thermal conductivity is still lacking.

If we assume that minerals with conductivities λ_i and volume concentrations V_i are arranged in parallel in a nonporous rock, then the thermal conductivity λ_s of the solid rock will be given by

$$\lambda_s = \frac{\sum \lambda_i V_i}{\sum V_i}. \quad (1)$$

When a low conductivity phase, such as a pore with porosity ϕ is present along with a solid phase of conductivity λ_s , there is equal probability of them occurring in series or in parallel. The resulting effective thermal conductivity λ_e takes the following form:

$$\lambda_e = \lambda_f \phi + \lambda_s (1 - \phi), \quad (2)$$

where λ_s and λ_f are the thermal conductivities of the rock and the fluid, respectively. This form gives the highest values of thermal conductivity of the rock/fluid system (λ_e) of all mixing-law models. The harmonic-mean model implies a series arrangement of the components;

$$\lambda_e = \left[\frac{\phi}{\lambda_f} + \frac{1 - \phi}{\lambda_s} \right]^{-1} \quad (3)$$

This model gives the lowest value of λ_e .

A modification of the weighted arithmetic-mean or parallel model, Eq. (2), is used by Sugawara and Yoshizawa [7] to obtain good agreement between their experimental and calculated thermal conductivities of two-phase, fluid-saturated rocks. This model is given by

$$\lambda_e = (1 - A)\lambda_s + A\lambda_f, \quad (4)$$

where A is an adjustable parameter that is defined by

$$A = \left[2^n (2^n - 1)^{-1} \right] \left[1 - (1 + \Phi)^{-n} \right]; \quad n > 0$$

Here, n is the empirical exponent depending on porosity, shape, orientation, and emissivity inside the pores.

The geometric-mean model [15] is

$$\lambda_e = (\lambda_f)^\Phi \lambda_s^{(1-\Phi)}. \quad (5)$$

The dispersive or extended Maxwell model has a thermal conductivity [2] given by

$$\lambda_e = \lambda_s \left[\frac{\left(\frac{2\lambda_s}{\lambda_f} + 1 \right) - 2\Phi \left(\frac{\lambda_s}{\lambda_f} - 1 \right)}{\left(\frac{2\lambda_s}{\lambda_f} + 1 \right) + \Phi \left(\frac{\lambda_s}{\lambda_f} - 1 \right)} \right]. \quad (6)$$

The first two models, Eqs. (2) and (3), have a firm physical basis, but are essentially special cases that are unrealistic in most practical situations. The weighted geometric-mean model, Eq. (5), has no physical basis. But since it is easier to use than Eq. (6) and gives similar results over the limited range of heat flow work, some authors prefer to use it.

The Maxwell model [17], which is the direct analog of the electrical case and has a good physical basis, gives quite reliable results when the porosity, ϕ , of one of the two components does not exceed about 0.25 and the thermal conductivity ratio ($r = \frac{\lambda_s}{\lambda_f}$) does not exceed 10.

2.2. Empirical Correlations

The effects of a number of physical properties on the thermal conductivity of several different dry sandstone samples have been investigated [18, 19], and the existence of several correlations between thermal conductivity, density, and porosity are reported, for example,

$$\lambda_e \propto \rho^4, \quad (7)$$

where λ_e is the thermal conductivity in $\text{W} \cdot \text{m}^{-1} \cdot \text{K}^{-1}$ and ρ is the bulk density. The bulk density is also correlated with the porosity as

$$\rho \propto (1 - \Phi), \quad (8)$$

and by substituting Eq. (8) into Eq. (7) one obtains

$$\lambda_e \propto (1 - \Phi)^4. \quad (9)$$

The proportionality constants may vary according to the origin of rocks. Extrapolations of empirical models to suites of rocks other than those used in developing the correlation equations may not be reliable.

3. EXPERIMENTAL TECHNIQUES AND SAMPLE CHARACTERIZATION

All the samples for thermal transport studies were obtained from Jhelum Khewra, with the collaboration of the Pakistan Natural History Museum Shakar Parian, Islamabad. The sandstone is about 156 m thick and displaced fine-grained to medium-grained sandstone, siltstone, shale, and occasional carbonates. The Khewra sandstones have been proved as oil reservoirs in some of the oil fields located in the Potohar areas of Pakistan.

Five samples were taken from different positions above the baseline (Table I) and were cut into specimens of rectangular shapes of $0.043 \times 0.045 \times 0.025 \text{ m}^3$. The thickness of the samples was chosen to satisfy the probing depth criteria [20] of thermal conductivity measurements. Each sample consists of two identical slabs. The surfaces of these samples were polished to provide good thermal contact with the transient plane source (TPS) sensor and to minimize thermal contact resistance. The mineral content was obtained by the thin-section technique and by chemical analysis. The density and porosity of the samples were (see Table I) measured by using American Society for Testing and Materials (ASTM) standard methods [21] and details have been published by the present authors [22]. The TPS technique was chosen to measure the thermophysical parameters because of the simplicity of the technique [23] and its applicability to insulators, fluids, metals [24], and superconductors [25]. This technique uses a resistive element (Fig. 1) as both a heat source and temperature sensor. To measure the thermal transport properties, a simple bridge circuit is used as shown in Fig. 2. By supplying a constant current to the TPS sensor (20 mm diameter) and by monitoring the subsequent voltage increase over a short period of time (after the start of the experiment), it is possible to get precise information about thermal transport properties of the material surrounding the heat source. Prior to transient recording, the bridge is balanced. Then a constant current pulse is passed through the TPS sensor, which changes the bridge to the off-balance mode. Under this condition, the time-dependent resistance of the TPS during the transient recording can be expressed, according to Ref. 26, as

$$R(t) = R_0 \left(1 + \beta \overline{\Delta T(\tau)} \right), \quad (10)$$

Table I. Characteristics of the Khewra Sandstones at Room Temperature and Atmospheric Pressure

Sample Type	Position above base line (m)	Color	Main lithology	Mineral content (vol.%)			
				Quartz	Calcite	Potassium feldspars	Dolomite
Kh SS1	26.4	Purple brown to dark brown	Silty shale to clay	54.9	5.7	5.2	34.2
Kh SS2	45.9	Light brown to greenish grey	Fine sandstone to dolomitic	59.5	2.5	5.6	32.5
Kh SS3	54.9	Grey	Silty sandy calcareous	64.5	4.3	4.0	27.2
Kh SS4	74.7	Brown to dark brown	Sandstone	77.0	4.1	2.8	16.2
Kh SS5	119.9	Reddish brown	Sandstone	71.4	6.2	2.5	19.8

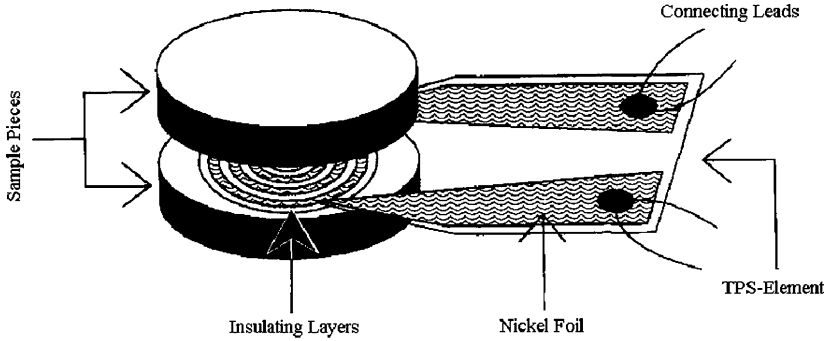


Fig. 1. Arrangement of the sample pieces with the TPS element.

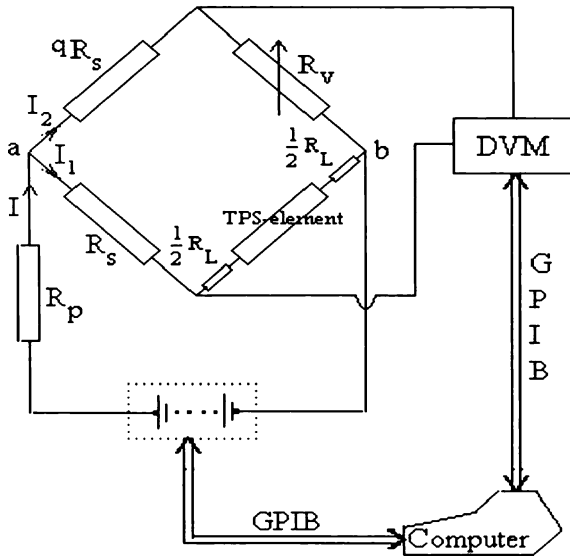


Fig. 2. Block diagram of the electrical bridge circuit along with the rest of the experimental setup, DVM, digital voltmeter, R_s , standard resistance, R_L , lead resistance, and R_p , series resistance.

where R_0 is the resistance of the TPS sensor before the start of transient recording, β is the temperature coefficient of resistivity of the TPS sensor, and $\Delta T(\tau)$ is the mean value of the temperature increase of the TPS sensor during the transient recording. In this equation the temperature change expressed as a function of the dimensionless variable τ , is defined by

$$\tau = (t/\theta)^{1/2}, \quad \theta = d^2/a, \tag{11}$$

where t is the time measured from the start of the transient heating, d is the measure of the overall size of the resistive pattern or the radius of the disk, a is the thermal diffusivity of the sample under test, and θ is the characteristic time.

The mean temperature change $\overline{\Delta T(\tau)}$ can be calculated by the solution of the basic heat conduction equation $a\nabla^2 T = \partial T / \partial t$ under non-steadystate conditions which gives the following results [23, 26] for the ring source solution:

$$\overline{\Delta T(\tau)} = P_0(\pi^{3/2}d\lambda)^{-1}D_s(\tau). \quad (12)$$

Equation (12) shows that $\overline{\Delta T(\tau)}$ depends on P_0 , the output power in to the TPS sensor, λ , the thermal conductivity of the material. The design parameter of the resistive pattern is denoted by $D_s(\tau)$. The resistance increase of the TPS sensor (Figs. 1 and 2) can be expressed as

$$\Delta R(t) = \beta R_0 \overline{\Delta T(\tau)}. \quad (13)$$

Substituting Eq. (12) in Eq. (13), we get

$$\Delta R(t) = \beta R_0 P_0 (\pi^{3/2} d \lambda)^{-1} D_s(\tau). \quad (14)$$

The relation with temperature changes in the TPS sensor, and the off-balance voltage variation of the bridge can be expressed via a third parameter $\Delta E(t)$ as

$$\Delta E(t) = R_s(R_s + R_0)^{-1} I_0 \Delta R(t), \quad (15)$$

where I_0 is the intensity of the constant current pulse measured across a $10\ \Omega$ standard resistance R_s . The bridge constant q (Fig. 2) in this experiment was kept equal to 100. However, one can adjust this ratio according to the experimental conditions. The constant current I_0 should be chosen such that the total temperature increase should be kept less than 1 K [23]. The scatter in the thermal conductivity measurements is about 0.14% and is about 0.66% and 0.52% in the thermal diffusivity and volumetric heat capacity measurements, respectively [26, 27].

By recording the voltage drop over a particular time interval, detailed information about the thermal conductivity, λ , and thermal diffusivity, a , of the test specimen is obtained. The heat capacity per unit volume, ρc_P , may be calculated from the relation, $\rho c_P = \frac{\lambda}{a}$.

All samples were dried at $105 \pm 5^\circ\text{C}$ for 8 h, then cooled down to room temperature, and finally kept in a desiccator. The thermal conductivity and thermal diffusivity of all the samples were measured as a function of temperature. Results are shown in Figs. 3 and 4. The thermal

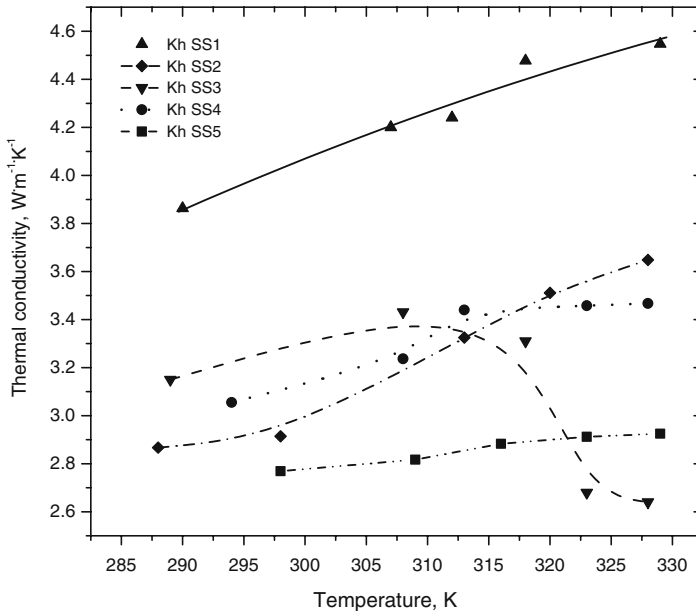


Fig. 3. Variation in thermal conductivity with temperature. Estimated uncertainties in λ_{exp} are about 6%.

conductivity and thermal diffusivity data are characterized by uncertainties of 6% and 8%, respectively [26]. The characteristics of the samples obtained by visual inspection, the main lithology, the mineral contents, and the position above the baseline are summarized in Table I.

4. RESULTS AND DISCUSSION

The measured porosity, density, and thermal conductivity at room temperature along with the calculated values of densities and effective thermal conductivities using various relations, are listed in Table II. The porosity and density of the samples were measured at 307 ± 1 K. The porosity of the samples varies from 8 to 17 vol.%. For a comparison of the experimental and calculated thermal conductivities, the conductivity data corresponding to the associated temperature will be considered.

Experimental results of the thermal conductivity and thermal diffusivity of the five sandstones as a function of temperature are shown in Figs. 3 and 4, respectively. The thermal conductivity of all five samples ranges between 2.82 and $4.20 \text{ W} \cdot \text{m}^{-1} \cdot \text{K}^{-1}$ at room temperature. The thermal conductivities of all sandstones under investigation increase slightly with temperature

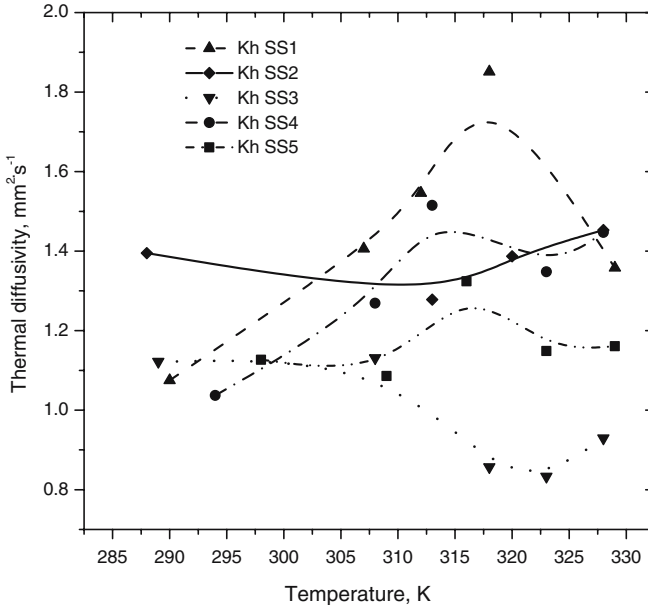


Fig. 4. Variation in thermal diffusivity with temperature. Estimated uncertainties in a_{exp} are about 8%.

except for Kh SS3, which decreases slightly. Both of these effects have already been observed in this type of sandstone [19]. The change in thermal diffusivity as a function of temperature is similar to that of the thermal conductivity, as it depends directly upon the thermal conductivity.

Figures 5 and 6 show the variation of the experimental thermal conductivity and thermal diffusivity of the five sandstones with porosity at 307 ± 1 K. Both the thermal conductivity and thermal diffusivity decrease with increasing porosity, which is in agreement with reported results [5, 16]. An increase in porosity results in a greater contribution from the pore filling and a decrease in the apparent density (Table II) and, hence, a reduction in the thermal conductivity. However, the minimum thermal conductivity cannot be smaller than that of the fluid in the pores.

For the estimation of λ_e , the mineral and air thermal conductivity values at room temperature were taken from Horai [28] and Zimmerman [6]: λ (air) = $0.026 \text{ W} \cdot \text{m}^{-1} \cdot \text{K}^{-1}$, λ (quartz) = $7.69 \text{ W} \cdot \text{m}^{-1} \cdot \text{K}^{-1}$, λ (calcite) = $3.59 \text{ W} \cdot \text{m}^{-1} \cdot \text{K}^{-1}$, λ (dolomite) = $3.34 \text{ W} \cdot \text{m}^{-1} \cdot \text{K}^{-1}$, and λ (potassium feldspar) = $2.31 \text{ W} \cdot \text{m}^{-1} \cdot \text{K}^{-1}$. All the samples are multi-mineral, with characteristic porosities ranging from 8 to 17 vol.%. Figure 7 shows comparisons of measured and predicted thermal conductivities of the samples as a function of porosity at 307 ± 1 K. Here, λ_e was calculated using

Table II. Experimental Porosity (ϕ), Density (ρ), and Thermal Conductivity (λ_{exp}) of Khewra Sandstones, along with the Predicted Density (ρ_e) and Effective Thermal Conductivities Calculated from Different Relations (Percentage deviations (% dev.) from ρ and λ_{exp} at normal temperature and pressure are also stated.)

Specimen	ϕ (vol.%)	ρ ($\text{kg} \cdot \text{m}^{-3}$)	$\rho_e = \rho_{\text{SiO}_2}$ ($1 - \phi$) ($\text{kg} \cdot \text{m}^{-3}$)	Stand. dev. (%)	λ_{exp} ($\text{W} \cdot \text{m}^{-1} \cdot \text{K}^{-1}$)	Stand. dev. (%)	$\lambda_e = \lambda_s$		Stand. dev. (%)	$\lambda_e = \lambda_s$ ($1 - \phi$) ⁴		Stand. dev. (%)
							$\lambda_e = \lambda_s$ $1 - \phi$	$\lambda_e = \lambda_s$ $1 - \phi$		$\lambda_e = \lambda_s$ $1 - \phi$	$\lambda_e = \lambda_s$ $1 - \phi$	
Kh SS1	8	2480	2438	1.7	4.20	1.21	4.01	4.5	4.08	3.0	3.0	
Kh SS2	11	2350	2358	0.3	3049	7.3	3.53	1.3	3.68	5.6	5.6	
Kh SS3	14	2190	2279	4.0	3.24	16.3	2.95	8.7	3.18	2.3	2.3	
Kh SS4	16	1950	2226	14.1	2.91	4.5	3.06	4.9	3.38	16.0	16.0	
Kh SS5	17	1750	2199	25.6	2.82	11.1	2.69	4.5	3.03	7.6	7.6	
Average		% dev.		9.2		10.3		4.8		6.9		

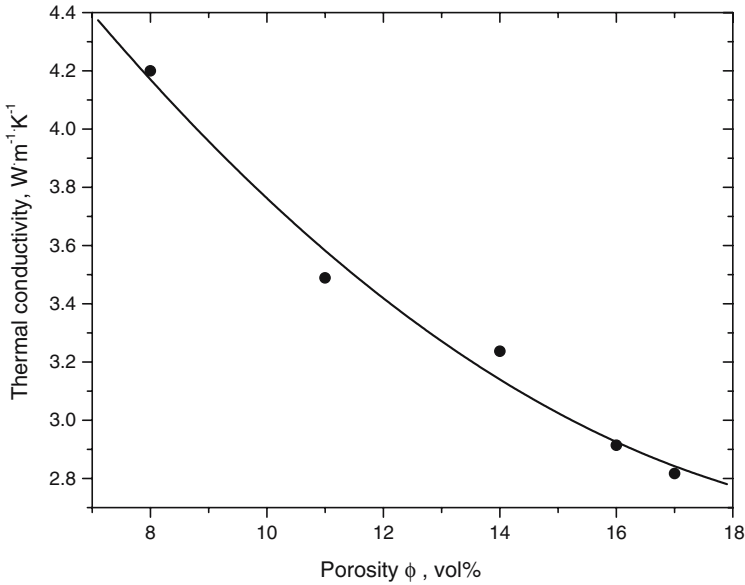


Fig. 5. Variation of measured thermal conductivity of five sandstones (see text) with change in porosity at 307 ± 1 K and at atmospheric pressure: (—), fitted by least-squares to second-order polynomial. Estimated uncertainties in λ_{exp} are 6%.

Eqs. (4), (5), and (9) and the thermal conductivity of the solid phase, λ_s , was determined from Eq. (1) with the use of the mineral content in each sample as stated in Table I. In estimating the value of λ_e , it is noticed that our experimental data give better agreement with the predicted thermal conductivities of the adjustable parameter A of Eq. (4), modified to

$$A = 2^2 \left[\frac{1}{(2-1)} \right] \left\{ 1 - \left[\frac{1}{(1+\phi)} \right] \right\}.$$

The decrease in thermal conductivity with increasing porosity is in agreement with previous observations [4, 15]. From Fig. 7 it is clear that the experimental and calculated thermal conductivities are in good agreement within experimental uncertainties. The Maxwell model could not be used for the prediction of λ_e because the ratio $\frac{\lambda_s}{\lambda_f}$ exceeds 10.

Figure 8 shows the variation in porosity with an increase in the position of the sample above the baseline, which again is in agreement with the observations. Figure 9 shows comparisons of the experimental and calculated thermal conductivities for the present work at 307 ± 1 K and atmospheric pressure. Good agreement exists, i.e., within experimental

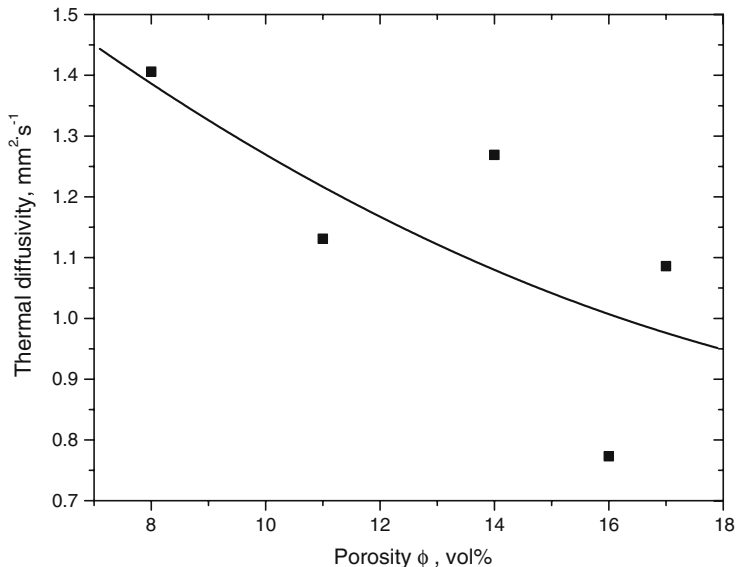


Fig. 6. Variation of measured thermal diffusivity of five sandstones (see text) with change in porosity at 307 ± 1 K and at atmospheric pressure: (—), fitted by least-squares to second-order polynomial. Estimated uncertainties in a_{exp} are 8%.

uncertainties. Further investigations into the effect of saturant, pore size, and pressure on the thermal transport properties should be carried out.

5. CONCLUSIONS

All the experiments were performed at atmospheric pressure with air as the fluid inside the pores. An important aspect of the TPS-method is the design of the TPS-elements, which are such that the TPS-elements can be used repeatedly and, furthermore, when comparing this technique with other methods such as the hot-wire [16] and transient hot-strip techniques [20], it must be remembered that the experiments are performed with very small temperature perturbations of the sample material. Under these circumstances, the agreement must be considered exceptionally good compared with any other method, particularly in view of the fact that the thermal conductivity, thermal diffusivity as well as volumetric heat capacity can be obtained from a single recording.

The density and the porosity of all the sandstones have been determined using the ASTM standard method at 307 ± 1 K. The experimental and calculated thermal conductivities of all the five sandstones as a

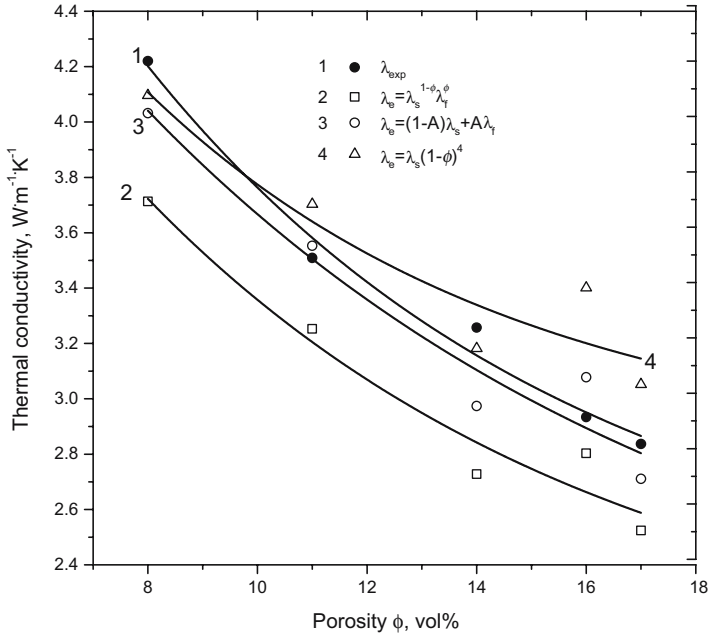


Fig. 7. Comparison of measured and calculated thermal conductivities of Khewra Sandstone (Kh SS) samples as a function of porosity at 307 ± 1 K.

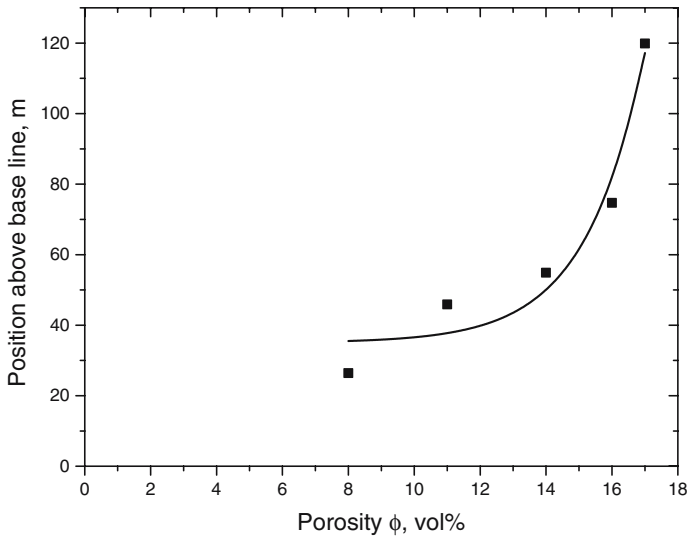


Fig. 8. Variation in porosity due to the position above the baseline.

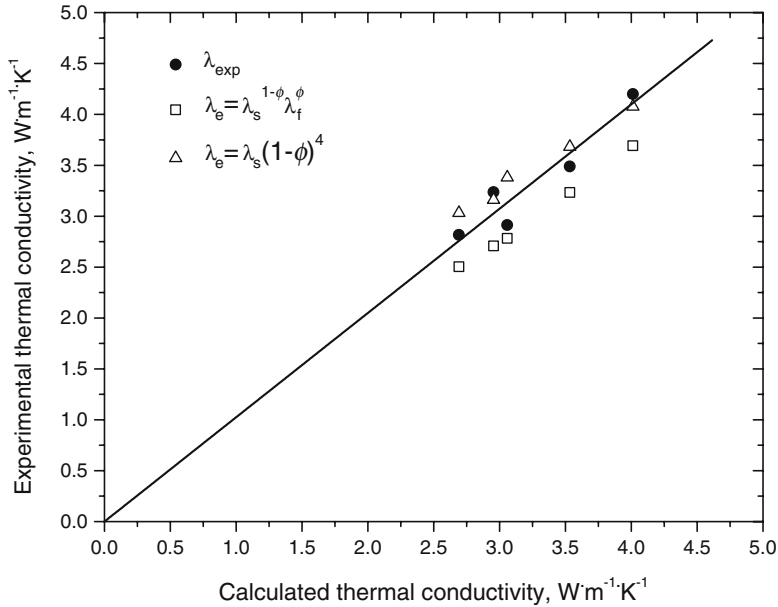


Fig. 9. Experimental thermal conductivity as a calculated function of effective thermal conductivity, calculated from different relations at 307 ± 1 K and atmospheric pressure.

function of porosity at 307 ± 1 K are in good agreement. For estimation of the thermal conductivity, the formula proposed by Sugawara and Yoshizawa [5] is slightly modified. It is also possible to predict the density of the samples by a simple relation with an average deviation of 10% from the experimental observations.

ACKNOWLEDGMENTS

The authors are grateful to the Higher Education Commission, Pakistan and Quaid-i-Azam University for supporting the present work financially. Dr. M. Anis-ur-Rehman and Mr. Iftikhar Hussain Gul are thanked for useful discussion on the subject. Mr. M. Bilal is acknowledged for providing some of the reference papers.

REFERENCES

1. F. Danes, B. Garnier, and T. Dupuis, *Int. J. Thermophys.* **24**:771 (2003).
2. A. E. Beck, *Geophysics* **41**:133 (1976).
3. W. D. Kingery, *J. Am. Ceram. Soc.* **42**:617 (1959).

4. W. H. Somerton, *Trans. AIME* **213**:61 (1958).
5. A. Sugawara and Y. Yoshizawa, *J. Appl. Phys.* **33**:3135 (1962).
6. R. W. Zimmerman, *J. Pet. Sci. Eng.* **3**:219 (1989).
7. A. Sugawara and Y. Yoshizawa, *Australian J. Phys.* **14**:468 (1961).
8. K. Lichtnecker, *Z. Phys.* **27**:115 (1926).
9. A. A. Babanov, *Sov. Phys. Tech. Phys.* **2**:476 (1957).
10. A. D. Brailsford and K. G. Major, *Br. J. Appl. Phys.* **15**:313 (1964).
11. J. Hutez, in *Progress in Heat and Mass Transfer*, Vol. 5 (Pergamon, Oxford, 1970).
12. V. Kummer and D. R. Chaudhary, *Ind. J. Pure Appl. Phys.* **18**:984 (1980).
13. R. N. Pande, V. Kumar, and D. R. Chaudhary, *Pramana* **22**:63 (1984).
14. K. Misra, A. K. Shrotriya, R. Singh, and D. R. Chaudhary, *J. Phys. D: Appl. Phys.* **27**:732 (1994).
15. K. J. Singh, R. Singh, and D. R. Chaudhary, *J. Phys. D: Appl. Phys.* **31**:163 (1998).
16. W. Woodside and J. H. Messmer, *J. Appl. Phys.* **32**:1688 (1961).
17. J. C. Maxwell, in *A Treatise of Electricity and Magnetism*, Vol. 1, 3rd Ed. (Clarendon, Oxford, 1904).
18. J. Anand, W. H. Somerton, and E. Gomma, *Soc. Petr. Eng. J.* **13**:267 (1973).
19. W. H. Somerton, in *Thermal Properties and Temperature Related Behaviour of Rock/Fluid Systems* (Elsevier, New York, 1992).
20. S. E. Gustafsson, E. Karawacki, and M. N. Khan, *J. Phys. D: Appl. Phys.* **12**:1411 (1979).
21. *Annual Book of ASTM Standard*, C20 (ASTM International, West Conshohocken, Pennsylvania, 1973).
22. A. Maqsood, M. A. Rehman, and I. H. Gul, *J. Chem. Eng. Data* **48**:1310 (2003).
23. S. E. Gustafsson, *Rev. Sci. Instrum.* **62**: 797 (1991).
24. A. Maqsood, N. Amin, M. Maqsood, G. Shabbir, A. Mahmood, and S. E. Gustafsson, *Int. J. Energy Res.* **18**:777 (1994).
25. M. Maqsood, M. Arshad, M. Zafarullah, and A. Maqsood, *Supercond. Sci. Technol.* **9**:321 (1996).
26. M. A. Rehman and A. Maqsood, *Int. J. Thermophys.* **24**:867 (2003).
27. M. A. Rehman and A. Maqsood, *J. Phys. D: Appl. Phys.* **35**: 2040 (2002).
28. K. Horai, *J. Geophysics Res.* **76**:1278 (1971).